ResearchGate

See discussions, stats, and author profiles for this publication at: https://www.researchgate.net/publication/41187906

Mapping of polymer melts onto liquids of soft-colloidal chains

ARTICLE *in* THE JOURNAL OF CHEMICAL PHYSICS · JANUARY 2010

Impact Factor: 2.95 · DOI: 10.1063/1.3292013 · Source: PubMed

CITATIONS
25

READS
12

2 AUTHORS:

Anthony Clark
Columbia University
11 PUBLICATIONS **85** CITATIONS
SEE PROFILE

Marina Guenza
University of Oregon
89 PUBLICATIONS **908** CITATIONS
SEE PROFILE

Available from: Marina Guenza
Retrieved on: 27 January 2016

Mapping of polymer melts onto liquids of soft-colloidal chains

A. J. Clark and M. G. Guenza[a)]
Department of Chemistry and Institute of Theoretical Science, University of Oregon, Eugene, Oregon 97403, USA

(Received 30 November 2009; accepted 17 December 2009; published online 26 January 2010)

Microscopic computer simulations of fluids of long polymers are greatly restricted by the limits of current computational power, and so course-grained descriptions, accurate on molecular length scales, are essential to extending the range of accessible systems. For some phenomena, particularly dynamical entanglement, descriptions that eliminate all internal degrees of freedom from the polymers are too drastic, as intermediate wavelength degrees of freedom are essential to the effect. Employing first-principles liquid-state theory, we have developed a course-grained model for the intermolecular structure of melts of long homopolymer chains that maps each chain of hard-sphere monomers onto a chain of connected soft colloids. All dependence on system parameters is analytically expressed so the results may be immediately applied to melts with different polymer and thermodynamic properties to calculate effective potentials between the soft colloids on the chains, which can then be used to perform molecular dynamics simulations. These simulations will be able to capture the large wavelength structure of the system at greatly reduced computational cost, while still retaining enough internal degrees of freedom explicitly to describe the phenomena that occur on length scales much larger than the monomeric units that comprise the chain, but shorter than the size of the molecule. © *2010 American Institute of Physics*.
[doi:10.1063/1.3292013]

I. INTRODUCTION

Liquids of polymers are of great importance in a variety of materials science and technological applications. Their structure is characterized by a wide range of relevant length scales, making the investigation of their properties particularly difficult. For both theoretical understanding of their properties and practical aspects of simulating realistic macroscopic systems within the limitations of available computational power, it is therefore important and desirable to formulate coarse-grained descriptions of the macromolecular liquid. These descriptions are accurate on large length scales, while irrelevant structural details on the short length scales are averaged out in order to give a computationally tractable system. Local scale information can be included *a posteriori* in the outcome of those simulations, either on the fly during the run of mesoscale simulations of coarse-grained systems, or after the coarse-grained simulations are completed through a multiscale modeling procedure.[1]

In our previous work we presented an analytical course-grained model that effectively maps a homopolymer melt onto a liquid of soft colloids. This model accurately reproduces the static structure of the melt on the molecular length scale and allows extensions of the range of systems that can be investigated through mesoscale simulations. In it, the polymers are described as point particles that interact via an effective pair potential with a range of the order of the polymer dimension, i.e., its radius of gyration R_g.[2,3] This large-scale model, combined with local scale united atom simulations, provides a complete description of the structure of the polymer melt at length scales between the bond length and R_g, and it is sufficient to give the needed information for liquids of unentangled macromolecules.[4]

However, some important phenomena that occur in polymer liquids take place on intermediate length scales, smaller than the size of the molecule, but still much larger than the size of the monomers. These phenomena include, for example, dynamical entanglements, blob chains for polymers dissolved in "good" solvents, and polymer pearl-necklace structures.[5,6] For systems where intermediate length scales are important, representing the polymer as one soft colloid is too drastic. Therefore it is necessary to develop a course-grained model that still averages out a large number of irrelevant degrees of freedom, to provide a reduction in required computation and make large-scale simulations of long-chain melts practical, while retaining enough effective internal degrees of freedom to describe internal structure on intermediate length scales.[7]

We present in this paper a model of this kind, where each chain is represented by a collection of identical shorter chains, so-called "blocks," connected together. Each short chain is mapped onto a point particle located at its center of mass, effectively replacing the long polymer by a chain of soft blocks. Because we treat homopolymer liquids, intra- and intermolecular interactions are identical. However, if the blocks in a chain were chemically different, the theory could be implemented to include repulsive or attractive interactions between blocks of different chemical nature, and the model would describe a liquid of coarse-grained block copolymers.[8]

Inputs to mesoscale simulations of coarse-grained systems are the effective potentials acting between effective units or blocks, which are calculated from the intermolecular

[a)]Electronic mail: mguenza@uoregon.edu.

 © 2010 American Institute of Physics

block-block (bb) pair distribution functions by enforcing a closure equation. Intermolecular pair distributions are derived from first-principles liquid-state theory using a generalized Ornstein–Zernike (OZ) equation where the monomeric units of the polymers are modeled as interacting rigid spheres. The course-grained description arises from adding imaginary, noninteracting sites fixed to lie at the center of mass of each block within each chain. The resulting equations can be solved to give analytical predictions in Fourier space for the pair correlations between block-center sites on different chains within the melt, allowing it to be immediately applied to a wide range of thermodynamic conditions and polymer types. Approximate analytical forms are then derived for the total pair correlations between blocks in real space. This contrasts with other course-graining schemes that have been applied to describe polymers as chains of soft colloids, which are numerical, and require simulations to be performed for each set of system parameters in order to determine effective potentials.[9]

The equilibrium intramolecular structure of polymers formed by distinct sub-blocks enters the generalized OZ equation. This includes all pair correlations involving monomers or block centers, which are formulated using the ideality of intrachain statistics for polymers in a melt. The Gaussian approximation for the block-monomer (bm) correlation, which was successful in representing the correlation between a site and block center previously for the soft-colloid[2,3] and diblock[8] models, still applies for subchains including a number of monomers higher than $N=30$ for relatively small numbers of blocks, but can lead to significant errors for blocks representing shorter subchains. We propose a more general approximation for the intermolecular correlation functions in real space, using the freely jointed chain model, which gives analytic dependence on system parameters, and can be extended naturally to different models of the intramolecular structure. Derived expressions for intra- and intermolecular monomer and block correlations throughout are compared with the United Atom Molecular Dynamics (UA-MD) simulations of a melt of 96 site polyethylene chains[10,11] with good agreement, supporting the validity of the proposed equations.

The paper is structured as follows. In the first section we present the generalized OZ equation for the coarse-graining of the homopolymer liquid into chains of soft blocks. Three sections follow in which we report the intramolecular monomer-monomer (mm), bm, and bb distribution functions. While the intramolecular Gaussian distribution works well for blocks of long chains, a more refined distribution is necessary for short blocks and for chains with a high number of blocks. We propose a freely jointed description which agrees well with data from united atom simulations. In the following three sections we present solutions for the total correlation functions between any combination of block and monomer pair interactions. An analytical solution for the freely jointed chain model shows improved agreement with simulation data when compared to the more traditional Gaussian distribution model. The improvement is more pronounced when the homopolymer is represented as a chain of short blocks, with a higher number of blocks.

II. GENERALIZED OZ EQUATION FOR BLOCK-LEVEL COARSE-GRAINING

The liquid-state approach introduced here represents a homopolymer as a chain of soft colloids or blocks. The block-level intermolecular correlations are derived following the solution of a generalized OZ equation where the monomer representation is described by real sites while the coarse-grained sites are fictitious. No direct correlation is present between fictitious sites or between real and fictitious sites.[12] This approach is an extension of our method to represent diblock copolymers as dumbbells of soft colloids of possible different chemical nature and/or degree of polymerization.[8] Our previous work also included a theory of coarse-grained homopolymers and their mixtures at the polymer center of mass (c.m.) level where the whole chain is represented as a single soft-colloidal particle.[2]

The new model introduced here describes homopolymer chains as a collection of an arbitrary number n_b of chemically identical blocks. Each block contains a number of sites N_b, such that $n_b \times N_b = N$, with N the total number of sites in a chain. Intra- and intermolecular total correlation functions are derived for each possible pairing of sites among the block c.m. and monomeric sites.

These intermolecular total correlation functions (TCFs) are of great relevance, since they are the starting point for the calculation of all the properties of interest, thermodynamic and dynamic, to describe the coarse-grained system. These include the effective potential between a pair of coarse-grained sites which is the necessary input to mesoscale simulations of the coarse-grained system. Because the effective potential is a free-energy, and therefore a function of the system parameters such as temperature, density, and degree of polymerization, different systems have different effective potentials. In this respect it is convenient to have analytical forms of the effective potentials, as are those in our treatment, because their parameter dependence is explicit, and they are directly applicable to different systems of interest, i.e., they are transferable.

The generalized OZ equation is formulated using the polymer reference interaction site model (PRISM). Extending the block-PRISM equations[13] by including fictitious sites which have no site-site direct correlation with other sites at the center of mass of each block, the resulting matrix equations are

$$\hat{\mathbf{h}}^{\mathrm{mm}(n_b)}(k) = \hat{\omega}^{\mathrm{mm}(n_b)}(k)\hat{\mathbf{c}}(k)(\hat{\omega}^{\mathrm{mm}(n_b)}(k) + N_b\rho_c\hat{\mathbf{h}}^{\mathrm{mm}(n_b)}(k)), \tag{1}$$

$$\hat{\mathbf{h}}^{\mathrm{bm}(n_b)}(k) = \hat{\omega}^{\mathrm{bm}(n_b)}(k)\hat{\mathbf{c}}(k)(\omega^{\mathrm{mm}(n_b)}(k) + N_b\rho_c\hat{\mathbf{h}}^{\mathrm{mm}(n_b)}(k)), \tag{2}$$

$$\hat{\mathbf{h}}^{\mathrm{mb}(n_b)}(k) = \hat{\omega}^{\mathrm{mm}(n_b)}(k)\hat{\mathbf{c}}(k)(\omega^{\mathrm{mb}(n_b)}(k) + N_b\rho_c\hat{\mathbf{h}}^{\mathrm{mb}(n_b)}(k)), \tag{3}$$

and

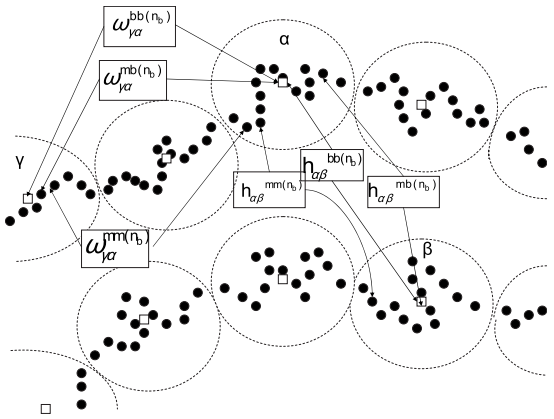

FIG. 1. Schematic illustration of the various block-averaged intramolecular and intermolecular distributions. Filled circles represent monomers and the open circles with dashed borders represent the effective soft sphere each block on the chain is mapped onto, and the c.m. of each block is represented by an open box.

$$\hat{\mathbf{h}}^{\mathrm{bb}(n_b)}(k) = \hat{\omega}^{\mathrm{bm}(n_b)}(k)\hat{\mathbf{c}}(k)(\omega^{\mathrm{mb}(n_b)}(k) + N_b\rho_c\hat{\mathbf{h}}^{\mathrm{mb}(n_b)}(k)). \tag{4}$$

Here ρ_c is the number density of chains. We denote correlations involving block-center sites by superscript b, and those involving real monomer sites by superscript m, and Greek indices are used to label the number of a block along a chain. The element $\hat{c}_{\alpha\beta}(k)$ denotes the direct correlation between the average monomer site on block α on one polymer and the average monomer site on block β on another. $\hat{\omega}_{\alpha\beta}^{\mathrm{mm}(n_b)}(k)$ is the intramolecular distribution between a monomer site on block α and a monomer site on block β of a given polymer, which has a number of blocks equal to n_b. The correlation between the block-center site on block α and a monomeric site on block β in the same chain is $\hat{\omega}_{\alpha\beta}^{\mathrm{bm}(n_b)}(k)$. An analogous formalism is adopted for the intermolecular TCFs; for example, $\hat{h}_{\alpha,\beta}^{\mathrm{bm}(n_b)}(k)$ is the correlation between the block-center site on block α and a monomeric site on block β on different chains. The intermolecular and intramolecular correlations that comprise these matrices are illustrated in Fig. 1.

All the sites inside one block are assumed to be equivalent. However, different blocks in the polymer remain distinguishable by their different distances from the end of the chain. To further clarify our treatment, we adopt for the bb matrix the following notation: $h^{\mathrm{bb}(n_b)}$ where n_b is the number of blocks included in the polymer. In this way, the generic matrix element $h_{ij}^{\mathrm{bb}(n_b)}$ expresses, for example, the position of block i inside a chain of n_b blocks, indicating if each block is central or terminal in the chain. This set of equations allows for the solution of the matrices $\hat{h}^{\mathrm{bb}(n_b)}(k)$, $\hat{h}^{\mathrm{bm}(n_b)}(k)$, and $\hat{h}^{\mathrm{mb}(n_b)}(k)$, which provides the block course-grained description of the polymer melt once the monomer level direct and intramolecular correlations are specified.

Assuming that all direct correlations are identical, since all monomers are identical, models of the system with different numbers of blocks can be related using only the intramolecular distributions. In particular, the soft colloid description can be recovered if the intramolecular distributions and any of the bb TCFs are known. For example, using the block-level TCF between an end block on each polymer, the soft colloid (one block) TCF is

$$\hat{h}^{\mathrm{bb}(1)}(k) = \left[\frac{\hat{\omega}^{\mathrm{bm}(1)}(k)}{\Sigma_{\gamma=1}^{n_b}\hat{\omega}_{\gamma}^{\mathrm{bm}(n_b)}(k)}\right]^2 \hat{h}_{11}^{\mathrm{bb}(n_b)}(k). \tag{5}$$

The one-block description recovers the equations for the c.m. derived in our previous papers,[2,3] given that $\hat{\omega}^{\mathrm{cm}}(k) \equiv \hat{\omega}^{\mathrm{bm}(1)}(k)$ and $\hat{h}^{\mathrm{cc}}(k) \equiv \hat{h}^{\mathrm{bb}(1)}(k)$ with the index c indicating the c.m. of the polymer. Here $\hat{\omega}^{\mathrm{cm}}(k)$ is the distribution of monomers about the polymer c.m. and $\hat{h}^{\mathrm{cc}}(k)$ is the TCF between the c.m. of two different chains.

III. INTRAMOLECULAR STRUCTURE

It is a long-established result that on large length scales, positions of monomeric units within a long polymer molecule in a melt follow, to very good approximation, the same statistical distribution as the steps in an unbiased, memoryless random walk, which is Gaussian. This behavior is due to the presence of forces from enough surrounding molecules to nearly cancel the excluded volume forces that would tend to swell the distribution, producing an "unperturbed" chain distribution.[6] Furthermore, local semiflexibility and barrier crossing become irrelevant when correlation functions describing the overall static structure of long polymers in a melt are under study, e.g., distributions of all sites about another site or point.[14] Finally, course-grained models of polymer systems, which are under study here, describe properties measured on length scales much larger than the monomeric units. For these models, the detailed properties of the interactions between monomers and their local conformational transitions are irrelevant because local degrees of freedom are averaged out, and the continuum Gaussian distribution becomes well justified.[5]

A. mm distributions

At the monomer level, the intramolecular structure factors in the Gaussian approximation for whole chains[5] and diblocks[15] are well known. Here we extend the model to a multiblock description of a homopolymer chain. In our notation, Greek indices are used to label the number of a block along a chain as before, and Latin indices are introduced to label the number of a site within that block, so that, for example, the ith site on the αth block is labeled by α_i. Consider two sites on different blocks, namely, α_i and β_j, where the blocks α and β satisfy the condition $\beta \geq \alpha$, and denote the statistical segment length as σ. The correlation between the two sites in a completely flexible polymer or in a semiflexible polymer on scale larger than the polymer persistence length, is given by

$$\hat{\omega}_{\alpha_i,\beta_j}^{\mathrm{mm}(n_b)}(k) = e^{-y(\sigma^2k^2/6)}. \tag{6}$$

In the block-site notation used here, y is given as $y = |j-i|$ for sites on the same block, while for different blocks, where $\alpha < \beta$, as $y = N_b + (\beta - \alpha - 1)N_b + j - i$. This counts the

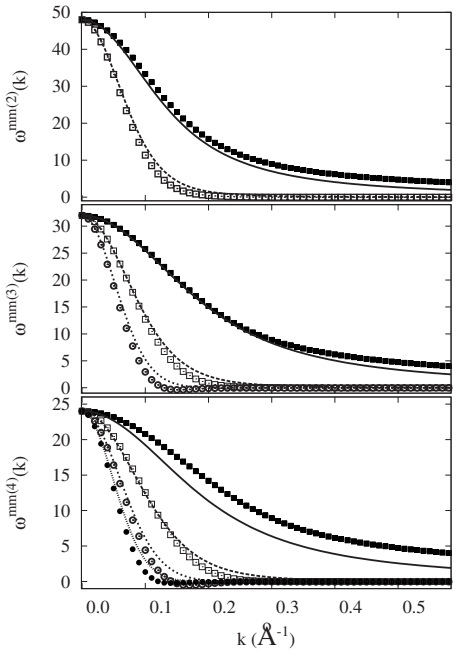

FIG. 2. Intramolecular site-site distributions for two, three, and four block models compared to polyethylene 96 simulation data. Predicted curves are shown for the possible block separations of the sites involved, with solid lines and filled boxes for sites on the same block, dashed lines and open boxes for sites on adjacent blocks, dotted lines and open circles for sites two blocks apart, and dotted-dashed lines and filled circles for sites three blocks apart. The range of wavevectors shown is from $k=0$ to the reciprocal of the statistical segment length $k=1/\sigma\approx 0.58377$ Å^{-1}.

chain steps from one block to an adjacent block with the first, i.e., N_b+1-i is the distance from site i to the first segment on the next block.

The average pair correlation between a site on block α and one on block β, which is input to Eqs. (1)–(3), is then

$$\hat{\omega}_{\alpha\beta}^{\mathrm{mm}(n_b)}(k)=\frac{1}{N_b}\sum_{i=1}^{N_b}\sum_{l=1}^{N_b}\hat{\omega}_{\alpha_i\beta_l}^{\mathrm{mm}(n_b)}(k). \tag{7}$$

In the continuum limit, Eq. (7) recovers for sites on the same block the equation for the undivided chain, but with the number of sites on the block in place of the number of sites on the chain. For sites on different blocks, however, a new form is obtained. Defining the radius of gyration of a block as $R_{gb}^2=N_b\sigma^2/6$ and adopting a new index $\gamma=|\alpha-\beta|$ to identify the number of blocks separating two sites, Eq. (7) reduces to

$$\hat{\omega}_{\alpha\beta}^{\mathrm{mm}(n_b)}(k)=\hat{\omega}_{\gamma}^{\mathrm{mm}(n_b)}(k)=\begin{cases}\dfrac{2N_b}{(kR_{gb})^4}(k^2R_{gb}^2-1+e^{-k^2R_{gb}^2}) & \text{if } \gamma=0,\\ \dfrac{N_b}{(R_{gb}k)^4}e^{-(\gamma-1)R_{gb}^2k^2}(1-e^{-R_{gb}^2k^2})^2 & \text{if } \gamma\neq 0.\end{cases} \tag{8}$$

For the case $n_b=2$ these reduce down to familiar results used in the context of diblock copolymers,[15] and for $n_b=1$ it reduces down to the overall chain result.[5]

To test the validity of our treatment, Fig. 2 shows the comparison between Eqs. (8) and data from a UA-MD simulation of polyethylene chains with a number of monomers per chain $N=96$ at $T=453$ K with density $\rho_c=3.28\times 10^{-2}$ Å^{-3}.[10] The value of the average block radius of gyration, used in the formulas above, is calculated from the radius of gyration of the chains measured in the UA-MD simulations, $R_g=281.70$ Å, by applying the relation $R_{gb}^2=R_g^2/n_b$.

Good agreement is observed for length scales much larger than the statistical segment length of the polymer, i.e., for $k\ll 1/\sigma\approx 0.583\,77$ Å^{-1} ("small" wavevectors), except for the same-block correlation in the $n_b=4$ case, where the block size ($N_b=24$) becomes so small that short-range and finite-chain effects start to dominate.

B. Distributions of monomers about block centers

Given the intramolecular pair correlation between site i on block β and the center of block α, $\hat{\omega}_{\alpha\beta_i}^{\mathrm{bm}}(k)$, the site-averaged distribution function is defined as

$$\hat{\omega}_{\alpha\beta}^{\mathrm{bm}}(k)=\sum_{i=1}^{N_b}\hat{\omega}_{\alpha\beta_i}^{\mathrm{bm}}(k). \tag{9}$$

In the case that the site and block center considered are on the same block, Eq. (9) recovers the single-chain distribution of sites around their c.m. The derivation of an analytical form for this quantity is well established,[14] and it is extended here to the case of different blocks $\alpha\neq\beta$.

Let us denote the vectors from the center site of block α to sites i on block α and j on block β as $\vec{S}_{\alpha\alpha_i}$ and $\vec{S}_{\alpha\beta_j}$, respectively. The bond vector from the ith site on the αth block to the next site $i+1$ on the chain is $\vec{r}_{\alpha_i}$. Assuming for convenience that $\beta>\alpha$, as the polymer chain is symmetric with respect to the center of the chain, we have

$$\vec{S}_{\alpha\beta_j}=\frac{1}{N_b}\sum_{i=1}^{N_b}\sum_{k=i}^{N_b}\vec{r}_{\alpha_k}+\sum_{\gamma=\alpha+1}^{\beta-1}\sum_{k=1}^{N_b}\vec{r}_{\gamma_k}+\sum_{k=1}^{j-1}\vec{r}_{\beta_k}, \tag{10}$$

where the first term represents the contribution related to the c.m. of the block α, the second term is the vector connecting block α to block β, and the third contribution gives the vector connecting to the site k on block β.

In the freely jointed chain model, where the probability distribution of finding a certain displacement between a pair of monomers is an isotropic Gaussian, the probability distribution of a sum of mm displacement vectors, such as the block c.m. distribution, will also be Gaussian. As a consequence, the probability of finding a site at a given distance from the block center is fully determined by the second moment of the Gaussian distribution. Because in this model different bond vectors are totally uncorrelated, $\langle\vec{r}_{\alpha_i}\cdot\vec{r}_{\beta_j}\rangle=\sigma^2\delta_{\alpha,\beta}\delta_{i,j}$, from Eq. (10) the second moment is found to be

$$\langle S_{\alpha\beta_j}^2\rangle=Q_{\alpha,\beta}^{(n_b)}+\frac{6}{N_b}(j-1)R_{gb}^2, \tag{11}$$

where

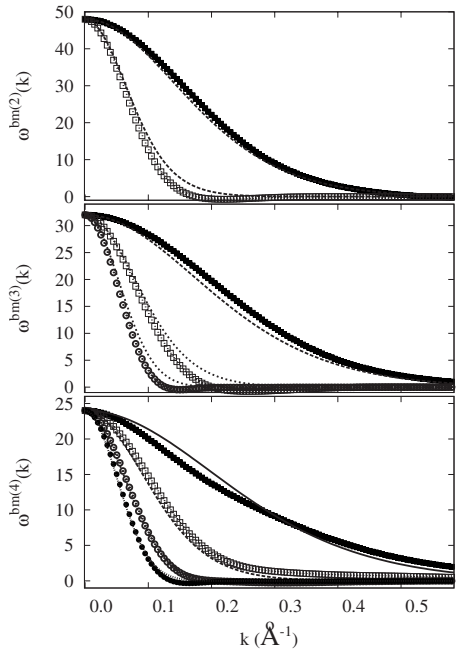

FIG. 3. Intramolecular block-center to site correlations for two, three, and four block models compared to simulation data of polyethylene with $N=96$. The notation and range of wavevectors are the same as in Fig. 2.

$$Q_{\alpha,\beta}^{(n_b)} \equiv 2\left(R_{gb}+\frac{1}{2N_b}R_{gb}\right)^2+\frac{3}{N_b}R_{gb}^2+6(\beta-\alpha-1)R_{gb}^2 - \frac{6}{N_b}R_{gb}^2 \approx 2R_{gb}^2+6(\beta-\alpha-1)R_{gb}^2.$$

The probability distribution of finding a site j on block β a distance from the center of block α corresponding to wave vector k, $\hat{\omega}_{\alpha\beta_j}^{\mathrm{bm}(n_b)}(k)$, is then given by

$$\hat{\omega}_{\alpha\beta_j}^{\mathrm{bm}(n_b)}(k)=e^{-\langle S_{\alpha\beta_j}^2\rangle k^2/6}, \tag{12}$$

which yields for the averaged quantity, with $\gamma=|\alpha-\beta|$ as before,

$$\hat{\omega}_{\alpha\beta}^{\mathrm{bm}(n_b)}(k)=\hat{\omega}_{\gamma}^{\mathrm{bm}(n_b)}(k) = \begin{cases} \left(\frac{N_b\sqrt{\pi}}{R_{gb}k}\right)\left(\mathrm{erf}\left[\frac{1}{2}kR_{gb}\right]\right)e^{-(R_{gb}^2k^2/12)} & \text{if } \gamma=0, \\ \frac{N_b}{k^2R_g^2}e^{-1/6[Q_{\gamma}^{(n_b)}k^2]}(1-e^{-R_{gb}^2k^2}) & \text{if } \gamma\neq 0. \end{cases} \tag{13}$$

In Fig. 3, Eqs. (13) are compared to data from the simulation of polyethylene melts with $N=96$. Again good agreement is observed for small k except for the same-block correlation in the $n_b=4$ with $N_b=24$ case. In this case, blocks are too short for their internal structure to be well approximated by this model, when correlations on the same block are calculated. However, monomer-block correlations follow the Gaussian statistics when the segment and the block-center are far apart on the same chain.

C. Pair distributions between block centers

It is important to calculate the intramolecular distributions between block centers in a chain, even if these quantities do not directly appear in the definition of the intermolecular TCFs, because they provide the needed formal background to calculate intramolecular effective potentials between blocks to be used as an input to molecular dynamics simulations of the block-coarse-grained polymer liquid.

Distributions for the separation of the centers of mass of a pair of blocks can be found by following an analogous procedure. The self-correlation of each block-center site is trivial $\hat{\omega}_{\alpha,\alpha}^{\mathrm{bb}}(k)=1$, so we focus only on the case $\alpha\neq\beta$. We denote the vector from the center of block α to the center of block β as $\vec{X}_{\alpha\beta}$. Because the distribution is Gaussian, only the second moment $\langle\vec{X}_{\alpha\beta}^2\rangle$ is needed to calculate the block-center properties of the system. The relative positions of the two-block centers can be written as linear combinations of Gaussian-distributed variables as $\vec{X}_{\alpha\beta}=\vec{S}_{\alpha\beta_j}-\vec{S}_{\beta\beta_j}$ for an arbitrary site, j, on block β. Using this definition and the result from the previous section for $S_{\alpha\beta_j}$ together with the known expression for $\vec{S}_{\beta\beta_j}$ (Ref. 14),

$$\vec{S}_{\beta\beta_j}=\frac{1}{N_b}\sum_{i=1}^{N_b}\left(\Theta(j-i)\sum_{l=i}^{j-1}\vec{r}_{\beta l}-\Theta(i-j)\sum_{l=j}^{i-1}\vec{r}_{\beta l}\right), \tag{14}$$

the second moment can be evaluated as

$$\langle\vec{X}_{\alpha\beta}^2\rangle=Q_{\alpha,\beta}^{(n_b)}+L, \tag{15}$$

with $L=R_{gb}^2(2(1-(5/N_b))(1-(1/N_b))+3((1/N_b)+(1/N_b^2))-(12/N_b^2))\approx 2R_{gb}^2$, and $Q_{\alpha,\beta}^{(n_b)}$ as defined previously. The distribution between a the block-center sites on blocks β and α (for $\alpha\neq\beta$) is

$$\omega_{\alpha\beta}^{\mathrm{bb}(n_b)}(k)=e^{-[(1/6)(Q_{\alpha\beta}^{(n_b)}+L)]k^2}. \tag{16}$$

The comparison of Eq. (16) against simulations of polyethylene $N=96$, displayed in Fig. 4, shows good agreement in the large-scale regime. The root mean square (rms) distance between adjacent block centers is predicted by this model to be $2R_{gb}$, while the end-block to end-block rms distance for asymptotically large numbers of blocks scales as $\sqrt{6n_b}R_{gb}=\sqrt{6}R_g$, recovering the end to end distance of the polymer predicted in the freely jointed chain model. This model therefore effectively maps the system onto a random walk with a step corresponding to each block.

In general, the predicted forms for all the intramolecular distributions show good agreement with the simulation data for small k, with larger deviations at larger wave vectors. The deviations at large wave vector are likely due to anomalous local-scale behavior, such as excluded volume effects due to finite monomer size and short range stiffness effects, that are neglected in this model.

Once the numerical inverse transform of the intramolecular forms is performed and data are compared with simulations, our formalism is found to accurately predict the intramolecular structure at large length scales, while a small deviation is observed at short length scales, as shown for the site to block-center correlations in a diblock model in Fig. 5. Because in a course-grained description detailed features on

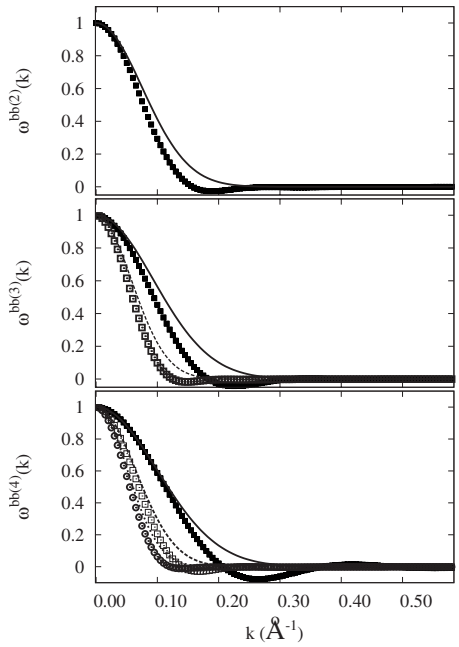

FIG. 4. Intramolecular correlations between block centers for two, three, and four block models compared to simulation data of polyethylene $N=96$. The notation and range of wavevectors are the same as in Fig. 2.

short length scales are averaged out, small local-scale deviations are irrelevant, and it is only necessary to accurately describe features on long length scales to obtain an accurate block-level description to be input to the OZ calculation of the intermolecular TCFs.

IV. SOLUTION OF THE INTERMOLECULAR TOTAL CORRELATION FUNCTIONS

The solution of the intermolecular TCFs must start from a series of approximations for the liquid structure at the monomer level. The bb correlation functions can be expressed in terms of the overall mm distribution, the bm intramolecular distributions, and the direct correlation function. The latter is assumed to be identical for all monomers on all blocks since all sites are chemically identical and interact by the same pair potentials.

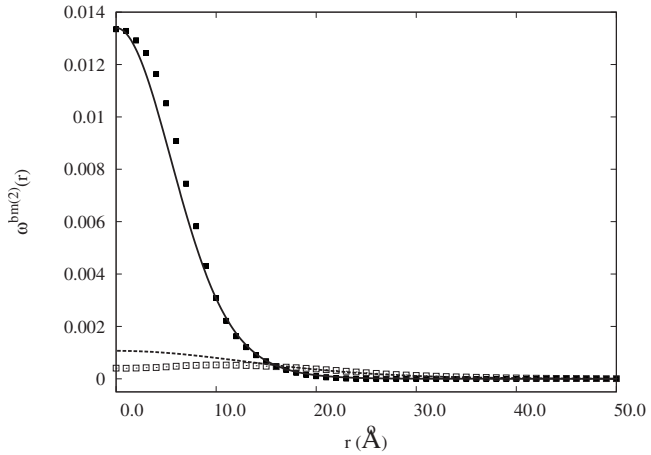

FIG. 5. Intramolecular correlations between sites and block centers in real space for two-block model: theoretical predictions (filled line) and simulations (filled squares) for sites and center on the same block; and theoretical predictions (dashed line) and simulations (open squares) for sites and center on different blocks.

For two blocks, correlations between any pair of blocks are indistinguishable

$$\hat{h}^{\mathrm{bb}(2)}_{\alpha\beta}(k) = \frac{\hat{c}(k)(\hat{\omega}^{\mathrm{bm}(2)}_0(k) + \hat{\omega}^{\mathrm{bm}(2)}_1(k))^2}{1 - N\rho_c\hat{c}(k)\hat{\omega}^{\mathrm{mm}(1)}(k)}, \tag{17}$$

where we used the fact that the overall chain intramolecular distribution $\hat{\omega}^{\mathrm{mm}(1)}(k)$, can be written in terms of the block-level intramolecular distributions as

$$\hat{\omega}^{\mathrm{mm}(1)}(k) = \frac{1}{n_b}\sum_{\alpha=1}^{n_b}\sum_{\beta=1}^{n_b}\hat{\omega}^{\mathrm{mm}(n_b)}_{\alpha\beta}(k). \tag{18}$$

The notation in Eq. (17) is the one defined for Eq. (8).

For three blocks and higher, distinct bb correlations occur due to the distinguishability of blocks depending on their distance from a chain end. Specifically for the three-block case, there are three distinct total correlations, as there are two end blocks and one interior block,

$$\hat{h}^{\mathrm{bb}(3)}_{11}(k) = \hat{h}^{\mathrm{bb}(3)}_{13}(k) = \hat{h}^{\mathrm{bb}(3)}_{31}(k) = \hat{h}^{\mathrm{bb}(3)}_{33}(k),$$
$$= \frac{\hat{c}(k)(\hat{\omega}^{\mathrm{bm}(3)}_0(k) + \hat{\omega}^{\mathrm{bm}(3)}_1(k) + \hat{\omega}^{\mathrm{bm}(3)}_1(k))^2}{1 - \hat{c}(k)N\rho_c(\hat{\omega}^{\mathrm{bm}(1)}(k))}, \tag{19}$$

$$\hat{h}^{\mathrm{bb}(3)}_{12}(k) = \hat{h}^{\mathrm{bb}(3)}_{23}(k) = \hat{h}^{\mathrm{bb}(3)}_{21}(k) = \hat{h}^{\mathrm{bb}(3)}_{32}(k),$$
$$= \frac{\hat{c}(k)(\hat{\omega}^{\mathrm{bm}(3)}_0 + 2\omega^{\mathrm{bm}(3)}_1)(\hat{\omega}^{\mathrm{bm}(3)}_0(k) + \hat{\omega}^{\mathrm{bm}(3)}_1(k) + \hat{\omega}^{\mathrm{bm}(3)}_2(k))}{1 - \hat{c}(k)N\rho_c(\hat{\omega}^{\mathrm{mm}(1)}(k))}, \tag{20}$$

and

$$\hat{h}_{22}^{\mathrm{bb}(3)}(k)=\frac{\hat{c}(k)(\hat{\omega}_0^{\mathrm{bm}(3)}(k)+2\omega_1^{\mathrm{bm}(3)}(k))^2}{1-\hat{c}(k)N\rho_c(\hat{\omega}^{\mathrm{mm}(1)}(k))}. \tag{21}$$

In general, for n_b blocks, the intermolecular TCF between blocks α and β, for $\alpha,\beta\leq(n_b+1)/2$ can be written

$$\hat{h}_{\alpha\beta}^{\mathrm{bb}(n_b)}(k)=\left(\frac{\hat{c}(k)}{1-\hat{c}(k)N\rho_c(\hat{\omega}^{\mathrm{mm}(1)}(k))}\right)\times\left(2\sum_{\gamma=0}^{\alpha-1}\Theta(\gamma)\hat{\omega}_\gamma^{\mathrm{bm}(n_b)}(k)+\Theta\left(\frac{2n_b-1}{4}-\alpha\right)\times\sum_{\gamma=\alpha}^{n_b-1}\hat{\omega}_\gamma^{\mathrm{bm}(n_b)}(k)\right)\times\left(2\sum_{\gamma=0}^{\beta-1}\Theta(\gamma)\hat{\omega}_\gamma^{\mathrm{bm}(n_b)}(k)+\Theta\left(\frac{2n_b-1}{4}-\beta\right)\sum_{\gamma=\beta}^{n_b-1}\hat{\omega}_\gamma^{\mathrm{bm}(n_b)}(k)\right), \tag{22}$$

where $\Theta(j)$ is the unit step function, defined such that $\Theta(0)=1/2$. All TCFs with $\alpha>(n_b+1)/2$ or $\beta>(n_b+1)/2$ can be found from these by the replacements $\alpha\rightarrow n_b-\alpha+1$ and $\beta\rightarrow n_b-\beta+1$, respectively.

In order to obtain analytical results using these forms, we employ the PRISM thread limit to determine the mm direct correlations, with the polymers treated as threads of vanishing thickness. The Percus–Yevick closure is applied for the hard core interactions between monomeric sites on different chains. The direct correlation is characterized by a single constant $\hat{c}(k)\rightarrow c_0$, and the intramolecular distributions reduced to analytically tractable continuum-limit results.

While giving only an average description of behavior on short length scales, this model provides an accurate description of the static structure on large length scales.[16] Since the course-grained approach is expected to be relatively insensitive to the details of structure on monomer length scales, the thread model is expected to be sufficiently accurate for this purpose while greatly simplifying the problem. Further justification for this approximation will be provided in a subsequent section.

A. Form of the bb total correlations in real space

To evaluate the quality of our newly derived expressions, we calculate the numerical Fourier transform of the total correlation functions, and directly compare them with the data from the united atom simulations.

The inverse Fourier transforms is defined as

$$h_\gamma^{\mathrm{bb}(n_b)}(r)=\frac{1}{2\pi^2 r}\int_0^\infty k\,\sin(kr)\hat{h}_\gamma^{\mathrm{bb}(n_b)}(k)dk. \tag{23}$$

The exact transforms, numerically calculated using Eq. (23), are reported in all the figures of TCFs for two and three blocks. They show good agreement with simulations within the numerical errors of the simulation analysis. More specifically, error estimates, shown at each point, are the standard deviation between the plotted histogram values and the surrounding values of a histogram with bins ten times smaller in width generated with the same data.

B. Approximate analytical forms for the block total correlation functions of a freely jointed chain

Consider the intermolecular TCFs as functions of the wavevector written in units of $1/R_{gb}$. All bb total intermolecular correlations for a chain with any number of blocks can be written in the generic form

$$\hat{h}^{\mathrm{bb}(n_b)}(k)=N_b\left(\frac{\hat{c}(k)\hat{B}(k)}{N_b^{-1}-\hat{c}(k)\rho_m\hat{W}(k)}\right), \tag{24}$$

where $\hat{c}(k)$ is the PRISM mm direct correlation function, N_b is the number of sites on each block, $\rho_m=N\rho_c$ is the density of monomers, and $\hat{W}(k)=\hat{\omega}^{\mathrm{mm}(1)}(k)/N_b$. $\hat{B}(k)$ is the combination of bm intramolecular distributions, appropriate for the particular number and combination of blocks involved, normalized by the number of sites per block. For example, for a diblock, $\hat{B}(k)=(\hat{\omega}_0^{\mathrm{bm}(2)}(k)/N_b+\hat{\omega}_1^{\mathrm{bm}(2)}(k)/N_b)^2$, and for the end blocks on a three-block chain $\hat{B}(k)=(\hat{\omega}_0^{\mathrm{bm}(3)}(k)/N_b+\hat{\omega}_1^{\mathrm{bm}(3)}(k)/N_b+\hat{\omega}_2^{\mathrm{bm}(3)}(k)/N_b)^2$.

Since the maximum values of the intramolecular distributions grow linearly with N_b, the functions $\hat{W}(k)$ and $\hat{B}(k)$ remain finite in the $N_b\rightarrow\infty$ limit. As functions of the rescaled wavevector, they reach a fixed form in this limit, $\lim_{N_b\rightarrow\infty}(\partial\hat{W}/\partial N_b)=\lim_{N_b\rightarrow\infty}(\partial\hat{B}/\partial N_b)=0$. Assuming that $\hat{c}(k)$ also remains finite and reaches a fixed form in this limit, $\lim_{N_b\rightarrow\infty}(\partial\hat{c}/\partial N_b)=0$, the leading-order expansion of the nonsingular part of $\hat{h}(k)$ in $1/N_b$ is

$$\hat{h}^{\mathrm{bb}(n_b)}(k)=N_b\left[-\frac{1}{\rho_m}\left(\frac{\hat{B}_\infty(k)}{\hat{W}_\infty(k)}\right)-\frac{1}{N_b\rho_m^2(\lim_{N_b\rightarrow\infty}\hat{c}(k))}\left(\frac{\hat{B}_\infty(k)}{(\hat{W}_\infty(k))^2}\right)\right], \tag{25}$$

where $\hat{B}_\infty(k)\equiv\lim_{N_b\rightarrow\infty}\hat{B}(k)$ and $\hat{W}_\infty(k)\equiv\lim_{N_b\rightarrow\infty}\hat{W}(k)$. This assumes of course that $\hat{W}_\infty(k)$ has no zeros at finite values of k, which is the case for the polymer model considered here.

The limits of the intramolecular distributions that make the $B(k)$ and $W(k)$ forms are exactly the continuum distributions found in the previous section. The limit of the direct correlation as $N_b\rightarrow\infty$, or equivalently as $N\rightarrow\infty$, expressed in real space in units of R_g, must be a function of vanishing width, when we assume that it remains of spatial range comparable to the size of an individual site. As the direct correlation is a reasonably well-behaved function, the limit should therefore be proportional to a δ distribution in real space, and therefore a constant in momentum space.

This is the thread model, wherein the form of the direct correlation $c(r)=c_0\delta(r)$, which has an analytical solution for hard-sphere sites given by $c_0=(1/N\rho_m)((\xi_c/\xi_\rho)-1)$ where the density screening length is $\xi_\rho=((\sqrt{2}/R_g)+(1/3)\pi\rho\sigma^3)^{-1}$,

the correlation hole length scale is $\xi_c = R_g/\sqrt{2}$, with the statistical segment length $\sigma = R_g/\sqrt{N}$.[16] Therefore, it gives in the limit of long chains $\lim_{N\to\infty} \hat{c}(k) = -2\pi^2\rho\sigma^6$.

Because the monomer-block center correlations fall off as Gaussians at large wavevectors, and the mm distributions fall off as k^{-2}, this series converges to arbitrary order and so arbitrarily accurate approximations could be formulated by keeping additional expansion terms. Since the purpose of this model is to describe long chains, we present here only the leading-order expansion.

If all higher derivatives of the direct correlations with respect to N are assumed to vanish in the asymptotic limit as well, the asymptotic series can be continued and converges to arbitrary order, and the use of the limiting forms of the distribution functions and monomer-level correlations is exact. Since the direct correlation parameter in the thread model and its value in the $N\to\infty$ limit differ by only a small amount for melts, the use of the thread-model monomer-level solution as input is well justified.

The inverse Fourier transforms of the TCF in Eq. (25) $\hat{h}^{\mathrm{bb}(n_b)}(s)$ is expressed as a function of the normalized separation distance $s = r/R_{gb}$, and can be written as

$$\hat{h}^{\mathrm{bb}(n_b)}(s) \approx -\frac{N_b}{2\pi^2 R_{gb}^3 \rho_m s}\int_0^\infty q\,\sin(qs)\left(\frac{\hat{B}_\infty(q)}{\hat{W}_\infty(q)}\right)dq + \frac{1}{4\pi^4 R_{gb}^3\sigma^6\rho_m^3 s}\int_0^\infty q\,\sin(qs)\left(\frac{\hat{B}_\infty(q)}{(\hat{W}_\infty(q))^2}\right)dq, \tag{26}$$

with $q \equiv kR_g$.

If the polymer chain is represented as one block, the c.m. TCF is

$$h^{\mathrm{bb}(1)}(s) = -\frac{N_b}{R_{gb}^3\rho_m}(Y_0^{(1)}(s)) + \frac{1}{2\pi^2 R_{gb}^3\sigma^6\rho_m^3 s}(Z_0^{(1)}(s)). \tag{27}$$

For two blocks

$$h^{\mathrm{bb}(2)}(s) = -\frac{N_b}{R_{gb}^3\rho_m}(Y_0^{(2)}(s) + 2Y_{01}^{(2)}(s;\eta_1) + Y_1^{(2)}(s;2\eta_1)) + \frac{1}{2\pi^2 R_{gb}^3\sigma^6\rho_m^3 s} \times (Y_0^{(2)}(s) + 2Y_{01}^{(2)}(s;\eta_1) + Y_1^{(2)}(s;2\eta_1)), \tag{28}$$

with η_γ defined as $\eta_\gamma = Q_\gamma/R_{gb}^2 \approx 6(\beta-\alpha)-4$, where β and α are the block indices as before.

The TCFs for a chain divided into a number of blocks higher than two are more involved but still straightforward to calculate. As an example, the TCFs for a three-block chain, which includes three different block combinations, are presented in the Appendix.

Here the Y and Z functions for the freely jointed chain model are defined as

$$Y_0^{(n_b)}(s) \equiv \frac{n_b}{2\pi s}\int_0^\infty q\,\sin(qs)\left(\frac{q^2\mathrm{erf}^2\left[\frac{1}{2}q\right]e^{-(1/6)q^2}}{2(n_bq^2 - 1 + e^{-n_bq^2})}\right)dq, \tag{29}$$

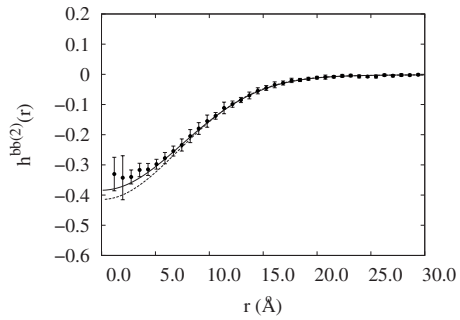

FIG. 6. Large-block approximation form (full line) for the intermolecular block-center to block-center distribution for the two-block model compared to polyethylene 96 simulations (symbols) and numerical inverse transform (dashed line).

$$Y_{01}^{(n_b)}(s;\mu) \equiv \frac{n_b}{2\pi^{3/2}s}\int_0^\infty q\,\sin(qs) \times\left(\frac{q\,\mathrm{erf}\left[\frac{1}{2}q\right]e^{-((1/12)+(1/6)\mu)q^2}(1-e^{-q^2})}{2(n_bq^2 - 1 + e^{-n_bq^2})}\right)dq, \tag{30}$$

$$Y_1^{(n_b)}(s;\mu) \equiv \frac{n_b}{2\pi^2 s}\int_0^\infty q\,\sin(qs)\left(\frac{e^{-(1/6)\mu q^2}(1-e^{-q^2})^2}{2(n_bq^2 - 1 + e^{-n_bq^2})}\right)dq, \tag{31}$$

and

$$Z_0^{(n_b)}(s) \equiv \frac{n_b^2}{2\pi s}\int_0^\infty q\,\sin(qs)\left(\frac{q^6\,\mathrm{erf}^2\left[\frac{1}{2}q\right]e^{-(1/6)q^2}}{4(n_bq^2 - 1 + e^{-n_bq^2})^2}\right)dq, \tag{32}$$

$$Z_{01}^{(n_b)}(s;\mu) \equiv \frac{n_b^2}{2\pi^{3/2}s}\int_0^\infty q\,\sin(qs) \times\left(\frac{q^5\,\mathrm{erf}\left[\frac{1}{2}q\right]e^{-((1/12)+(1/6)\mu)q^2}(1-e^{-q^2})}{4(n_bq^2 - 1 + e^{-n_bq^2})^2}\right)dq, \tag{33}$$

and

$$Z_1^{(n_b)}(s;\mu) \equiv \frac{n_b^2}{2\pi^2 s}\int_0^\infty q\,\sin(qs)\left(q^4\frac{e^{-(1/6)\mu q^2}(1-e^{-q^2})^2}{4(n_bq^2 - 1 + e^{-n_bq^2})^2}\right)dq. \tag{34}$$

Note that the Y and Z functions depend only on the number of blocks n_b. Because the dependence on all the system parameters (ρ, N_b, and R_{gb}) is expressed in the analytical prefactors, once the number of blocks n_b is defined, our formalism can be directly applied to any polymer melt of interest, including more accurate descriptions of semiflexibility, polymer architecture, and possibly even good solvent conditions, without the need to rederive approximations.

Figures 6 and 7 show that this "large block" approximation works well for any case under study. Reasonable agreement is seen even for three blocks where $N_b = 32$ and chains start to be too short to obey random statistics. The result of keeping the second order term in $1/N_b$ is also shown for the three-block case to demonstrate that the deviations from the

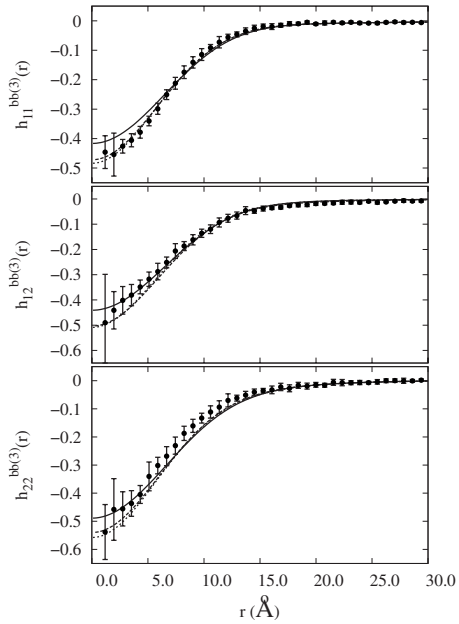

FIG. 7. Large-block approximation forms to leading order (full line), and second order (dotted line) form for the intermolecular block-center to block-center distribution for the three-block model compared to polyethylene 96 simulations (symbols) and numerical inverse transform (dashed line).

exact result, observed at small separation for the first order form, are overcome when the second order correction is included. This shows that deviations of our freely jointed chain solution from the exact numerical result are due solely to the relatively small number of sites on each block ($N_b=32$).

C. Analytical total correlation functions in the Gaussian approximation

While the approximate solution for the coarse-grained liquid of freely jointed chains gives predictions in quantitative agreement with the exact (numerical) result of the inverse transform integral [Eq. (23)], and simulations, in this section we want to compare the quality of agreement observed in this model against our traditional Gaussian model, which we have adopted in our previous papers.[2,3,8] The Gaussian model provides an analytical formalism for the TCFs and effective potentials, in quantitative agreement with simulations, when polymer chains are represented as soft-colloidal particles or soft-colloidal dumbbells.

Extending the traditional Gaussian approach for diblock copolymer course-graining,[8] we assume that all intramolecular bm distributions are Gaussian. The total correlations can then be written in terms of a simple, analytical functional form, derived in the original coarse-graining analysis of polymer melts.

The Gaussian approximation, for a chain divided into n_b blocks, takes the form

$$\hat{\omega}_{\gamma}^{\mathrm{bm}}(k) \approx N_b e^{-Y_{n_b,\gamma}k^2}, \tag{35}$$

with $Y_{n_b,\gamma}=R_{n_b,\gamma}^2/6$. Here $R_{n_b,\gamma}$ is the calculated average separation of sites between a block center and sites on a block which is γ blocks away. Using this together with the standard Padè approximation to the Debye form for the overall mm intramolecular distribution, $\hat{\omega}^{\mathrm{mm}(1)}(k)\approx N/(1+\xi_c^2k^2)$, and the definition of the density screening length (in the thread limit) $\xi_\rho=\xi_c/\sqrt{(1-\rho_c c_0)}$, the total correlations can be expanded into sums over terms of the form[2,3,8]

$$\hat{T}_0(k;X) = \left(\frac{N_b^2 c_0 \xi_\rho^2}{\xi_c^2}\right)\frac{(1+\xi_c^2k^2)e^{-Xk^2}}{1+\xi_\rho^2k^2}, \tag{36}$$

where X is a sum of two of the $Y_{n_b,\gamma}$ parameters defined previously. The inverse transform of Eq. (36) is given by

$$\begin{aligned} T_0(r;X) = {} & \frac{1}{8\pi^{3/2}}\left(\frac{\xi_c^2}{\xi_\rho^2}\right)e^{-(r^2/4X)} + \frac{1}{8\pi\xi_\rho^2}\left(\frac{\xi_c^2}{\xi_\rho^2}-1\right) \\ & \times\frac{e^{X/\xi_\rho^2}}{r}\left(e^{r/\xi_\rho}\,\mathrm{erfc}\left[\frac{\sqrt{X}}{\xi_\rho}+\frac{r}{2\sqrt{X}}\right]\right. \\ & \left. - e^{-r/\xi_\rho}\,\mathrm{erfc}\left[\frac{\sqrt{X}}{\xi_\rho}-\frac{r}{2\sqrt{X}}\right]\right). \end{aligned} \tag{37}$$

For two blocks the total correlation functions are simply given by

$$\begin{aligned} h^{\mathrm{bb}(2)}(r) = {} & \frac{N_2^2 c_0 \xi_\rho^2}{\xi_c^2}(T_0(r;2Y_{2,0}) + T_0(r;2Y_{2,1}) \\ & + 2T_0(r;Y_{2,0}+Y_{2,1})), \end{aligned} \tag{38}$$

where $h_{11}^{\mathrm{bb}(2)}=h_{12}^{\mathrm{bb}(2)}=h_{21}^{\mathrm{bb}(2)}=h_{22}^{\mathrm{bb}(2)}$.

For three blocks the three distinct correlations become

$$\begin{aligned} h_{11}^{\mathrm{bb}(3)} = {} & \frac{N_3^2 c_0 \xi_\rho^2}{\xi_c^2}(T_0(r;2Y_{3,0}) + T_0(r;2Y_{3,1}) + T_0(r;2Y_{3,2}) \\ & + 2T_0(r;Y_{3,0}+Y_{3,1}) + 2T_0(r;Y_{3,0}+Y_{3,2}) \\ & + 2T_0(r;Y_{3,1}+Y_{3,2})), \end{aligned} \tag{39}$$

$$\begin{aligned} h_{12}^{\mathrm{bb}(3)} = {} & \frac{N_3^2 c_0 \xi_\rho^2}{\xi_c^2}(T_0(r;2Y_{3,0}) + 2T_0(r;2Y_{3,1}) \\ & + 3T_0(r;Y_{3,0}+Y_{3,1}) + T_0(r;Y_{3,0}+Y_{3,2}) \\ & + 2T_0(r;Y_{3,1}+Y_{3,2})), \end{aligned} \tag{40}$$

$$\begin{aligned} h_{22}^{\mathrm{bb}(3)} = {} & \frac{N_3^2 c_0 \xi_\rho^2}{\xi_c^2}(T_0(r;2Y_{3,0}) + 4T_0(r;2Y_{3,1}) \\ & + 4T_0(r;Y_{3,0}+Y_{3,1})). \end{aligned} \tag{41}$$

Similar forms can be written for higher numbers of blocks, and they are not reported here. Using the definition of $c_0=(1-\xi_c^2/\xi_\rho^2)/N\rho_m$ and $\xi_\rho'\equiv 3/(\pi\rho_c\sigma^2)=N/(2\pi\rho_c R_g^2)$ to eliminate the density, we recover for the two blocks the form

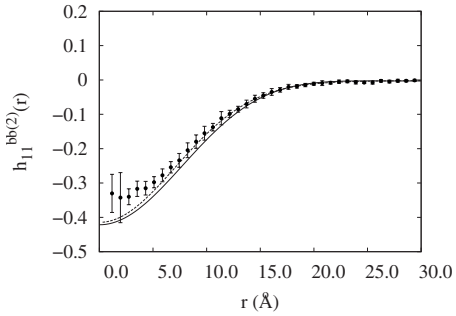

FIG. 8. Gaussian approximation for intermolecular block-center to block-center distribution for the two-block model (full line) compared to the polyethylene 96 simulations (symbols) and numerical transform of exact derived form (dashed line).

derived previously in the context of diblock copolymers.[8] When compared with simulation data, the Gaussian formalism shows good but less quantitative agreement than the freely jointed chain approximation which is more precise.

Figures 8 and 9 show the Gaussian approximation compared to exact results and polyethylene simulation data for the two and three-block models. The Gaussian approximation shows increasing deviation from the numerically derived form and from simulation data for three blocks. This suggests the need for a more accurate approximation, such as the proposed freely jointed chain formalism, when chains containing more than two blocks are under study.

In our previous papers on homopolymer and diblock copolymer course-graining, the intramolecular distributions of monomers about fictitious center sites was successfully approximated using the Gaussian function. The Gaussian approximation works well for these models because it is a very good description of the distribution at small wave vectors (large length scales), which dominate the total correlations

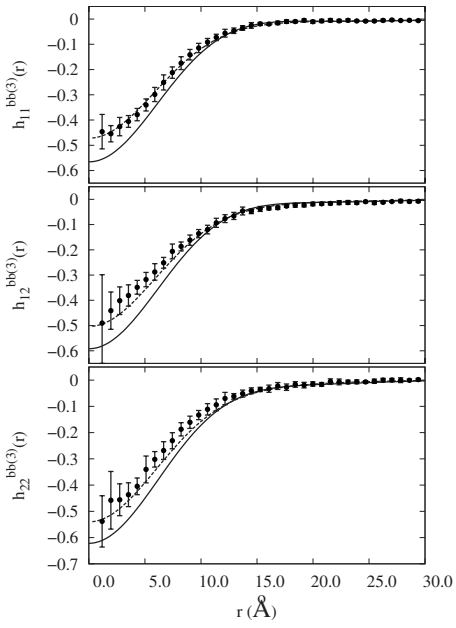

FIG. 9. Gaussian approximation for intermolecular block-center to block-center distribution for the three-block model (full line) compared to the polyethylene 96 simulations and numerical transform of exact derived form (dashed line).

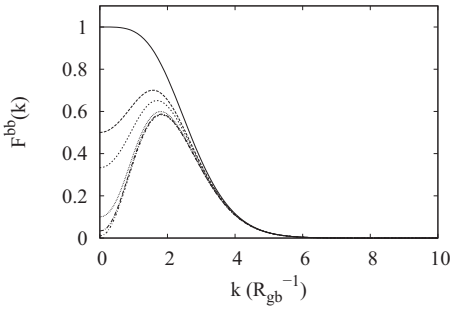

FIG. 10. Functional form of the $F^{bb}(k)$ contribution to the TCF for fixed block length for chains comprised of several numbers of blocks shows that the function is increasingly dominated by a peak at nonzero wavevector. Similar behavior is observed for other terms that contribute to the TCFs for large numbers of blocks. Shown are one (solid line) two (long-dashed line), three (short-dashed line), ten (dotted line), 30 (long-dash-dotted line), and 100 (short-dashed-dotted line) blocks.

for large chains with a small number of blocks. However, its accuracy decreases on larger wave vectors as more blocks are added to each chain; our study suggests that in this case the total correlations between block centers come to depend more and more on the intermediate wave vector values of the intramolecular distribution, causing the total correlation to suffer increasing contribution on short length scales from the region of the Gaussian distribution considered unreliable, i.e., large k regime.

To demonstrate this effect, consider the functional form in momentum space of the contribution to the lowest order asymptotic expansion form of the TCF $\hat{h}^{bb(n_b)}(k)$ given in Eq. (25) that arises from correlations between real monomers that are on the same block as the block center site involved for both chains, $\hat{F}^{bb}(k) \propto ((\omega_0^{bm(n_b)})^2(k)/\omega^{mm(1)}(k))$. Using the continuum freely jointed chain correlations and explicitly writing the chain radius of gyration in terms of the block radius of gyration, the result for various numbers of blocks is given by

$$\hat{F}^{bb}(k) \equiv \frac{n_b \pi (R_{gb}k)^2 \,\mathrm{erf}^2\left[\frac{1}{2}R_{gb}k\right]}{2(n_b(R_{gb}k)^2 - 1 + \exp[-n_b(R_{gb}k)^2])}. \tag{42}$$

Figure 10 shows this function versus wavevector for chains with increasing numbers of blocks with the length of each block fixed. As the number of blocks is increased, the maximum of the function moves from $k=0$ to a value just below $k=2/R_{gb}$. The contribution of this term to the total correlation in real space therefore is increasingly composed of values at wavevectors away from $k=0$. Other terms arising from contributions to the TCFs due to sites on different blocks show a similar onset of intermediate-wavevector dominance that starts at higher numbers of blocks, leading to the overall result for the total bb TCF to become increasingly sensitive to the intermediate-wavevector values of the distribution of sites about the block center. For this reason approximations formulated for accuracy at very small wavevectors such as the Gaussian approximation (for length scales long compared to the block radius) should be expected to yield increasing error for larger numbers of blocks.

V. CONCLUSION

We have presented a model based on first-principles, microscopic liquid-state theory that provides a complete description of structure on the length scales of long sub-blocks on long homopolymer chains in a melt. The model gives analytic forms, which allow it to be applied directly to a wide variety of different polymer types and thermodynamic conditions. It is capable of describing effects within a polymer that occur on length scales which are smaller than the size of the polymer but much larger than the size of the monomers it is comprised of, while still providing a dramatic degree of simplification over full monomer-level models.

This fills a gap between the drastic molecular course-graining model previously outlined where a polymer chain was represented as a soft-colloidal particle, and monomer-level descriptions. The single soft colloid representation has the disadvantage that it cannot be used to describe processes that occur on shorter length scales than the molecular size, while many interesting phenomena in polymer physics occur on the submolecular lengthscale, i.e., entanglement constraints. Our coarse-graining model overcomes the limitations of the monomer-level models, for which the needed computational power makes simulating large systems impossible, while still allowing for relevant degrees of freedom within each molecule to be retained. While no simulations in the entangled regime have been performed here, our model gives the static effective interactions between polymers that will be a necessary input for mesoscale simulations of entangled systems, providing an important first step toward performing such simulations in future.

The advantage of our multiblock model with respect to other models present in the literature is that our formalism contains an explicit dependence on the molecular and thermodynamic parameters of the system. For this reason our effective potential is readily applicable to different polymeric systems. The derived effective potentials will be used in future work to map a homopolymer melt onto a fluid of short coarse-grained interacting chains. This should allow for the extension of the range in time and length scales where polymer liquids and composites can be simulated further into the regime of long chains, where multichain entanglement significantly effects the dynamics of the system.

ACKNOWLEDGMENTS

We acknowledge the support of the National Science Foundation through Grant No. DMR-0804145.

APPENDIX: THREE-BLOCK TOTAL CORRELATION FUNCTIONS FOR A FREELY JOINTED CHAIN MODEL

Three-block TCFs for the freely jointed chain model are simply calculated following the procedure described in the paper:

$$h_{11}^{\mathrm{bb}(3)}(s) = -\frac{N_b}{R_{gb}^3\rho_m}(Y_0^{(3)}(s) + 2Y_{01}^{(3)}(s;\eta_1) + 2Y_{01}^{(3)}(s;\eta_2) + 2Y_1^{(3)}(s;\eta_1+\eta_2) + Y_1^{(3)}(s;2\eta_1) + Y_1^{(3)}(s;2\eta_2)) + \frac{1}{2\pi^2 R_{gb}^3\sigma^6\rho_m^3 s}(Z_0^{(3)}(s) + 2Z_{01}^{(3)}(s;\eta_1) + 2Z_{01}^{(3)}(s;\eta_2) + 2Z_1^{(3)}(s;\eta_1+\eta_2) + Z_1^{(3)}(s;2\eta_1) + Z_1^{(3)}(s;2\eta_2)), \tag{A1}$$

$$h_{12}^{\mathrm{bb}(3)}(s) = -\frac{N_b}{R_{gb}^3\rho_m}(Y_0^{(3)}(s) + 3Y_{01}^{(3)}(s;\eta_1) + Y_{01}^{(3)}(s;\eta_2) + 2Y_1^{(3)}(s;\eta_1+\eta_2) + 2Y_1^{(3)}(s;2\eta_1)) + \frac{1}{2\pi^2 R_{gb}^3\sigma^6\rho_m^3 s}(Z_0^{(3)}(s) + 3Z_{01}^{(3)}(s;\eta_1) + Z_{01}^{(3)}(s;\eta_2) + 2Z_1^{(3)}(s;\eta_1+\eta_2) + 2Z_1^{(3)}(s;2\eta_1)), \tag{A2}$$

and

$$h_{22}^{\mathrm{bb}(3)}(s) = -\frac{N_b}{R_{gb}^3\rho_m}(Y_0^{(3)}(s) + 4Y_{01}^{(3)}(s;\eta_1) + 4Y_1^{(3)}(s;2\eta_1)) + \frac{1}{2\pi^2 R_{gb}^3\sigma^6\rho_m^3 s}(Z_0^{(3)}(s) + 4Z_{01}^{(3)}(s;2\eta_1) + 4Z_1^{(3)}(s;2\eta_1)). \tag{A3}$$

The Y and Z functions for the three-block freely jointed chain model are given by Eqs. (29)–(34).

The resulting functions are compared with exact numerical calculations using the thread model monomer theory and united atom simulations in Fig. 7, and show good agreement within the numerical error of the simulation statistics. Some deviation from the exact form is observed using the leading-order expansion due to the smallness of the number of monomers on each block (N_b=32). As evidence of this, the asymptotic expansion to second order in $1/N_b$ is shown as well, showing that the series still converges toward the exact expression.

[1] *Novel Methods in Soft Matter Simulations*, Lecture Notes Physics Vol. 640, edited by M. Karttunen, I. Vattulainen, and A. Lukkarinen (Springer-Verlag, Berlin, 2004).
[2] G. Yatsenko, E. J. Sambriski, and M. G. Guenza, J. Chem. Phys. **122**, 054907 (2005).
[3] G. Yatsenko, E. J. Sambriski, M. A. Nemirovskaya, and M. Guenza, Phys. Rev. Lett. **93**, 257803 (2004).
[4] J. McCarty, I. Y. Lyubimov, and M. G. Guenza, J. Phys. Chem. B **113**, 11876 (2009).
[5] M. Doi and S. F. Edwards, *The Theory of Polymer Dynamics* (Oxford University, Oxford, 1986).
[6] P.-G. de Gennes, *Scaling Concepts in Polymer Physics* (Cornell University Press, Ithaca, 1979).
[7] J. T. Padding and W. J. Briels, J. Chem. Phys. **117**, 925 (2002).
[8] E. J. Sambriski and M. G. Guenza, Phys. Rev. E **76**, 051801 (2007).
[9] A. Rakshit and R. C. Picu, J. Chem. Phys. **125**, 164907 (2006).

[10] D. Heine, D. T. Wu, J. G. Curro, and G. S. Grest, J. Chem. Phys. **118**, 914 (2003).
[11] E. Jaramillo, D. T. Wu, G. S. Grest, and J. G. Curro, J. Chem. Phys. **120**, 8883 (2004).
[12] V. Krakoviack, J. P. Hansen, and A. A. Louis, Europhys. Lett. **58**, 53 (2002).
[13] E. F. David and K. S. Schweizer, J. Chem. Phys. **100**, 7784 (1994).
[14] H. Yamakawa, *Modern Theory of Polymer Solutions* (Harper & Row, New York, 1971).
[15] M. Guenza, H. Tang, and K. S. Schweizer, J. Chem. Phys. **108**, 1257 (1998).
[16] K. S. Schweizer and J. G. Curro, Chem. Phys. **149**, 105 (1990).